# Superabsorbent Polymeric Materials. XIV. Preparation and Water Absorbency of Nanocomposite Superabsorbents Containing Intercalated Hydrotalcite

**Wen-Fu Lee, Yung-Chu Chen**

*Department of Chemical Engineering, Tatung University, Taipei, Taiwan, Republic of China*

Received 2 April 2004; accepted 12 July 2004
DOI 10.1002/app.21182
Published online 22 October 2004 in Wiley InterScience (www.interscience.wiley.com).

**ABSTRACT:** A series of novel xerogels, based on sodium acrylate (NaA), intercalated hydrotalcite (IHT), and *N,N′*-methylene-bisacrylamide (NMBA), were prepared by inverse suspension polymerization. The influences of the HT intercalated with acrylic acid (AA–IHT) and with 2-acryloylamido-2-methyl propane sulfonic acid (AMPS–IHT), the content of the IHT in the poly(NaA) gel on the water absorbency, and the initial absorption rate in deionized water and various salt solutions were investigated. Results showed that adding a small amount of IHT could effectively increase the water absorbency of the gels, but adding excess IHT could decrease the water absorbency of the gels. In addition, the water absorbency of the gels containing AA–IHT was lower than that containing AMPS–IHT. The initial absorption rate, for the present gels, increased with increasing content of IHT in the copolymeric gels. © 2004 Wiley Periodicals, Inc. J Appl Polym Sci 94: 2417–2424, 2004

**Key words:** superabsorbents; clay; hydrotalcite; gels; nanocomposites

## INTRODUCTION

Superabsorbents can absorb a large amount of water compared with general water-absorbing materials, in which the absorbed water is hardly removable even under some pressure. Because of their excellent characteristics, superabsorbents have generated considerable interest and research and have been used in the fields of health, agriculture, and horticulture.[1–4] The first superabsorbent polymer was reported by the U.S. Department of Agriculture in 1961,[5] and a number of researchers have since attempted to modify these absorbent polymers to enhance their absorbency, gel strength, and absorption rate.[6–20]

Hydrotalcite (HT) is composed of positively charged layers and interlayer-exchangeable anions.[21,22] Their general composition can be represented as $[Mg_{1-x}Al_x(OH)_2]^{x+}[CO_{3\,x/2}^{2-}\cdot nH_2O]$, where $Mg^{2+}$ and $Al^{3+}$ are divalent and trivalent cations, respectively, and $CO_3^{2-}$ is an exchangeable anion. In recent years, HT has received considerable attention because of its application as catalysts, ion exchangers, absorbents, ceramic precursors, and organic–inorganic nanocomposites.[23–29] In this study, HT was chosen as an inorganic filler to prepare hydrotalcite/polymer nanocomposite hydrogels.

In the past ten years, most research on nanocomposites focused on the use of silicate clays as nanoparticles.[30,31] The clays have been widely studied because they are naturally occurring minerals that are commercially available, and exhibit a platy morphology with a high aspect ratio and considerable cation-exchange capacity. Although many reports about the intercalation of organic anions into HT have been published,[32] relatively few reports have discussed the incorporation of HT into polymers. These studies on HT/polymer nanocomposites were mainly focused on intercalating and performance of these HT nanocomposites has been relatively seldom reported.

From our laboratory the effects of HT, on physical properties and drug-release behavior for nanocomposite hydrogels based on poly[acrylic acid-*co*-poly(ethylene glycol methyl ethyl acrylate)] (AA-*co*-PEGMEA)/HT gels, have been reported.[33] The results showed that the swelling ratio for the gels increased with increase in HT content. Incorporating intercalated-HT (IHT) into superabsorbent polymer and fabricating a composite is significant in reducing the product cost and improving the water absorbency of the superabsorbent materials. In this study, the HT intercalated by acrylic acid (AA) and 2-acryloylamido-2-methyl propane sulfonic acid (AMPS) was used to prepare poly(sodium acrylate)/IHT nanocomposites. The intercalation of AA or AMPS into HT promotes more hydrophilic HT nanolayers, enabling them to be

*Correspondence to:* W.-F. Lee (wflee@ttu.edu.tw).
Contract grant sponsor: Tatung University, Taipei, Taiwan; contract grant number: B91-1413-01.

**TABLE I**
**Feed Compositions and Yield of SA/Intercalated-Hydrotalcite Xerogels Obtained from Inverse Suspension**

| Sample code | SA (g) | AMPS–HT (g) (wt %) | AA–HT (g) (wt %) | NMBA (g) | Yield (%) |
|---|---|---|---|---|---|
| S0 | 20 | 0 | 0 | 0.07 | 92.3 |
| S1 | 20 | 0.202 (1) | — | 0.07 | 91.4 |
| S3 | 20 | 0.606 (3) | — | 0.07 | 90.5 |
| S5 | 20 | 1.010 (5) | — | 0.07 | 89.7 |
| S7 | 20 | 1.414 (7) | — | 0.07 | 90.4 |
| A1 | 20 | — | 0.202 (1) | 0.07 | 90.7 |
| A3 | 20 | — | 0.606 (3) | 0.07 | 93.8 |
| A5 | 20 | — | 1.010 (5) | 0.07 | 87.6 |
| A7 | 20 | — | 1.414 (7) | 0.07 | 89.6 |

exfoliated by acrylate molecules and to generate the exfoliated poly(acrylate)/IHT nanocomposites.

Additionally, another important reason for the adoption of AA or AMPS as intercalated species is that the reaction between the vinyl groups of the intercalated AA or AMPS and vinyl groups of the acrylate generates crosslinks between the IHT nanolayers and acrylate molecules, imparting greater compatibility of the exfoliated poly(acrylate)/IHT. Consequently, exfoliated poly(acrylate)/IHT nanocomposites, with excellent compatibility, are expected to show significantly improved water absorbency and absorption rate over those of pristine poly(acrylate). This article discusses the influence of different anionic intercalating agents for preparing poly(acrylate)/IHT nanocomposites and reports on the investigation of the effect of the content of intercalated-HT on the water absorbency of the nanocomposite superabsorbent.

## EXPERIMENTAL

### Materials

Acrylic acid (AA) was purified by vacuum distillation at 63°C/25 mmHg. Hydrotalcite (HT) and the crosslinker *N,N′*-methylene-bis-acrylamide (NMBA) were purchased from Aldrich (Milwaukee, WI). The anion-exchange capacity (AEC) of HT was about 350 meq/100 g. Sodium hydroxide and 2-acryloylamido-2-methyl propane sulfonic acid (AMPS) were purchased from Fluka Chemie (Buchs, Switzerland). 4,4′-Azobis(4-cyanovaleric acid) (ACVA), used as an initiator, and sorbitan monostearate (Span 60), used as a stabilizer, were purchased from Tokyo Kasei Industries Ltd. (Tokyo, Japan). Methanol and cyclohexane were of reagent analytical grade.

### Preparation of NaA monomer solution

NaA monomer was prepared as reported previously.[34]

### Intercalation of HT

The suspension solution containing 5 g of HT and 3.24 g of AMPS or 1.26 g of AA was mixed in 500 mL of *N,N′*dimethylacetamide. The suspension solution was stirred at 70°C for 24 h, then the intercalated HT was separated by centrifugation and washed with large volumes of water to remove unintercalated AMPS. The sample was dried in a vacuum oven at 40°C for 3 days. The obtained IHT was designated as AA–IHT and AMPS–IHT for AA and AMPS intercalation, respectively.

### Preparation of sodium acrylate and IHT nanocomposite superabsorbent polymer by inverse suspension polymerization (ISP)

A 300-mL four-neck separable flask, equipped with a reflux condenser, a stirring rod, and a thermometer, was charged with 65 mL cyclohexane and 0.2 g Span 60. The mixture was stirred until Span 60 was dissolved (continuous phase).

The crosslinking agent NMBA and the appropriate amount of AA–IHT or AMPS–IHT, were introduced into NaA monomer solution and the mixture was stirred until the NMBA was dissolved completely. The monomer solution and 0.15 g of the initiator ACVA (dispersion phase) were introduced into the reactor. Air was flushed from the reactor by introducing nitrogen until the entire process was completed. The stirrer speed was maintained at 500 rpm. The polymerization was set at 70°C for 4 h. After polymerization, the suspension solution was cooled and then precipitated by 800 mL cold methanol under stirring. The product was filtered and washed several times by the mixture of water and methanol (1 : 9 v/v). The product was then dried in a vacuum oven at 100°C for 1 day. A white powdered polymer was obtained. The feed compositions of samples are listed in Table I.

### Measurement of property

All samples were dried in a vacuum oven at 100°C before any tests. All of the samples were used with a particle size in the range of 65–100 mesh.

### X-ray diffraction (XRD) analysis

Powder XRD analyses were performed by using a MAC Science X-ray powder diffractometer with Cu

anode (model M21X, Osaka, Japan), running at 40 kV and 30 mA, scanning from 2 to 13° at 3°/min. The structure of the HT was determined at different stages of the nanocomposite synthesis. The HT powders were mounted on a sample holder with a large cavity and a smooth surface was obtained by pressing the powders with a glass plate. Analyses of the HT swollen in the gels were performed by spreading the mixture on a gel membrane disc (50 mm diameter, 0.5 mm thick) used as sample holder. It was designed so that a maximum surface could be irradiated at low angle, giving an optimum intensity to the XRD signal. The nanocomposite plates, produced during the molding process, had a fairly smooth surface.

### Morphology

The dried specimens were examined for morphological details by using scanning electron microscopy (SEM; model JXA8600, JEOL, Tokyo, Japan) at an acceleration voltage of 15 kV. The specimens were coated with a gold metal layer to provide proper surface conduction.

### FTIR analysis

Fourier transform infrared spectra were recorded from pressed KBr pellets containing about 1% of the HT and intercalated HT, respectively, using a Horiba FTIR-720 spectrophotomer (Kyoto, Japan).

### Zeta-potential analysis

The dried IHT (30 mg) was immersed in 20 mL of deionized water. The zeta potential of the HT was measured by using a Zeta-Meter 3.0+ instrument (Zeta-Meter, Inc., Staunton, VA).

### Measurement of water absorbency

Suction filtration method

Each sample (50 mg) was immersed in an excess of deionized water or 0.9 wt % $NaCl_{(aq)}$ for at least 8 h to reach swelling equilibrium at room temperature and the residual water was removed by suction filtration with an aspirator (250 mmHg) for 15 min. The gel was weighed and the equilibrium absorbency $Q_{eq}$ was calculated by use of the following equation:

$$Q_{eq} = \frac{W_{wet} - W_{dry}}{W_{dry}} \quad (1)$$

where $W_{dry}$ is the weight of the dried sample and $W_{wet}$ is the weight of the swollen sample.

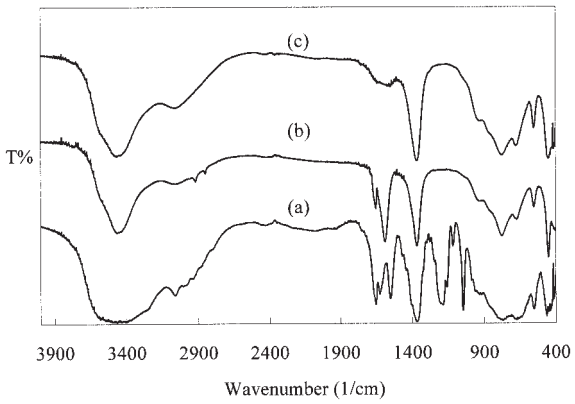


**Figure 1** FTIR spectrum of (a) AMPS–HT, (b) AA–HT, and (c) HT.

Tea-bag method

The tea bag was made of 250-mesh nylon screen. The tea bag containing the sample (50 mg) was immersed entirely in deionized water or the saline solution and kept there to attain swelling equilibrium, then hung up for 25 min to drain the excess solution, and weighed. The equilibrium absorbency was calculated by eq. (1).

### Absorbency in various saline solutions

Each sample (50 mg) was immersed in an excess of various saline solutions with different concentrations [$NaCl_{(aq)}$, $CaCl_{2(aq)}$, $FeCl_{3(aq)}$] and retained there for at least 8 h. The samples were filtered with suction and weighed. The water absorbency in each saline solution was obtained.

### Kinetics of swelling

The swelling kinetics was measured by the demand wettability (DW) method reported in previous related studies.[34,36]

## RESULTS AND DISCUSSION

### FTIR analysis

FTIR spectra of HT and IHT are shown in Figure 1. Strong absorption peaks, of asymmetric and symmetric R-$COO^{-1}$ groups, appear at 1610 and 1375 $cm^{-1}$, respectively. The characteristic absorption peaks of C═O stretching, C═C stretching, N—H bending, and S═O asymmetric stretching and S═O symmetric stretching appear at 1658, 1630, 1558, 1205, and 1049 $cm^{-1}$, respectively. These peaks demonstrate that AMPS was intercalated into the HT layer [see Fig. 1(a)]. The characteristic absorption peaks of C—O stretching and C═C stretching appear at 1656 and

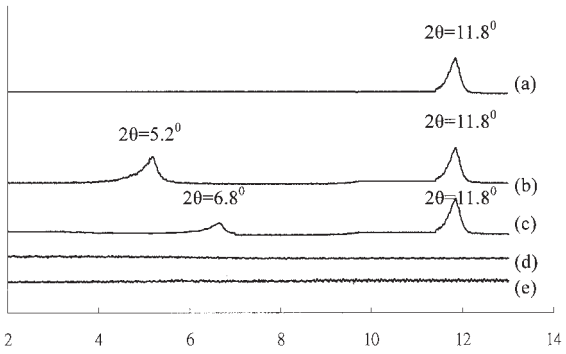


**Figure 2** XRD patterns of (a) HT, (b) AMPS–HT, (c) AA–HT, (d) S7, and (e) A7.

1600 $cm^{-1}$, respectively. These peaks demonstrate that AA was intercalated into the HT layer [see Fig. 1 (b)]. A broad absorption peak, between 3200 and 3600 $cm^{-1}$, is assigned to O—H stretching of both the hydroxide layers and the interlayer water.

### Identification of the nanocomposite hydrogels

XRD patterns for HT, AMPS–HT, AA–HT, and some typical samples, are shown in Figure 2. Before treatment with AMPS and AA, the carbonate group is an interlayer exchangeable anion in pure HT. A typical XRD pattern of HT, with a strong peak corresponding to a basal spacing of 7.49 Å, is shown in Figure 2(a). After treatment with AMPS, a new peak appeared, corresponding to basal spacing of 16.97 Å, as shown in Figure 2(b). This result shows that AMPS is intercalated between the layers during the anion-exchange process, adopting a lateral bilayer structure. For AMPS–HT, two peaks appear at $2\theta = 5.2°$ and $2\theta = 11.8°$, which indicates that both AMPS and carbonate groups are present in the interlayer galleries of AMPS–HT. As can be observed from the result in Figure 2(b), the equivalent content of carbonate group is approximately equal to that of AMPS. Therefore, AMPS does not completely exchange carbonate groups. After treatment with AA, a new peak appeared, corresponding to basal spacing of 12.98 Å, as shown in Figure 2(c). For AA–HT, two peaks appear at $2\theta = 6.8°$ and $2\theta = 11.8°$, which indicates that both AA and carbonate groups are present in the interlayer galleries of AA–HT. From results shown in Figure 2(c), one can see that the AA content is far less than the carbonate group content. Thus, we know that the anionic exchange ability of the AMPS was higher than that of the AA. The XRD pattern, for the gel series containing different IHT contents, did not exhibit any diffraction at $2\theta = 3$–$13°$, a result that suggests that the diffraction peak in both S- and A-series gels disappeared in all samples, such as S7 and A7 sample gels. This result demonstrated that the intercalated HT incorporated into the gels was completely exfoliated.

### Effect of IHT content on water absorbency in deionized water

The water absorbency in deionized water, measured by suction filtration and the tea-bag method, as a function of the content of IHT in the copolymeric gels is shown in Figure 3 (S-series and A-series). The results show that the water absorbency increases with increasing weight percentage of IHT when the value is <3 wt %. According to Flory's swelling theory,[35] water absorbency for the gel is dependent on the affinity of the gel toward water: there was a maximum effect of affinity for 3 wt % IHT. At >3 wt % the effect of affinity on IHT diminished, and the water absorbency depended on the amount of NaA of the copolymeric gels. For this reason, adding a small amount of the hydrophilic monomer IHT into the copolymeric gels can increase the affinity of the gels for water, and the water absorbency increased. However, at molar ratios > 3 wt %, the greater the content of IHT, the lower the water absorbency, although it remained higher than that of pure NaA. This is because the $[Mg_{1-x}Al_x(OH)_2]^{x+}$ nanolayers were exfoliated and well dispersed in the polymer matrix, causing more $[Mg_{1-x}Al_x(OH)_2]^{x+}$ nanolayers to form and providing a stronger hydration ability of the OH group. This leads to the nanocomposite hydrogels becoming more hydrophilic. Hence, the water absorbency increased with increasing content of IHT in the gel.[33] However, when the content of IHT is >3 wt %, the carboxylate groups on SA readily ionize and inter- or intramolecular ionic bonding occurs between anionic gel and cationic IHT nanolayers. Hence, the anionic charge density becomes lower in the gels at higher content of IHT.

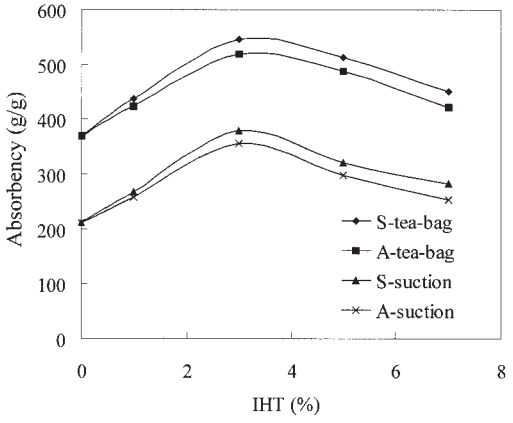


**Figure 3** Effect of AMPS–HT content and AA–HT content for the poly(SA/IHT) gels on absorbency in deionized water by tea-bag method and suction method.

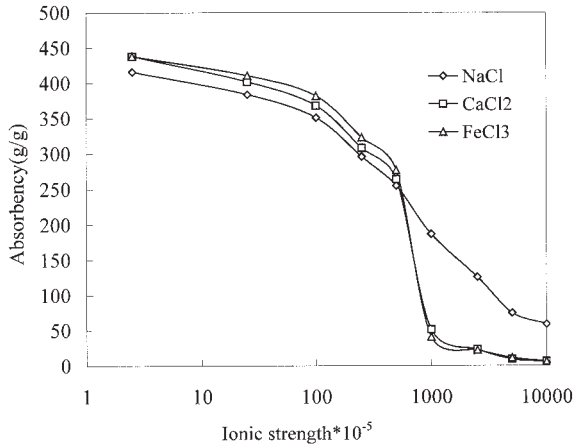


**Figure 4** Water absorbency of 3 wt % sample for the poly(SA/AMPS–HT) gels in $NaCl_{(aq)}$, $CaCl_{2(aq)}$, and $FeCl_{3(aq)}$ with various ionic strengths.

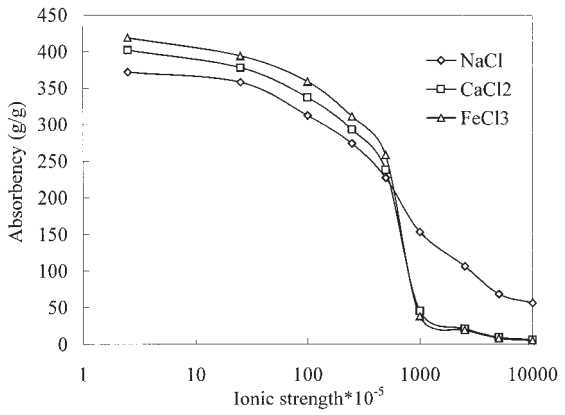


**Figure 5** Water absorbency of 3 wt % sample for the poly(SA/AA–HT) gels in $NaCl_{(aq)}$, $CaCl_{2(aq)}$, and $FeCl_{3(aq)}$ with various ionic strengths.

According to Flory's swelling theory,[35] decreasing the fixed charge of the polymer network could decrease the absorbency. In addition, Wu et al.[36] suggested that the clay powder could act as an additional network point. Hence, the higher the amount of clay powder, the greater the crosslinking density of the composite. As a result the gel network space becomes smaller and the water absorbency thus gradually decreases. The results also indicate that the water absorbency of the A-series gels was lower than that of the S-series gels. This is because the affinity of AA toward water was lower than that of AMPS, and the accompanying absorbency effect of multigroups ($SO_3^-$, $COO^-$) is larger than the absorbency effect of the single group ($COO^-$). Another reason was that the anionic charge density of the A-series gels was lower than that of the S-series gels. Because the zeta potential of AMPS–HT (+37.5 mV) was lower than AA–HT (+42.7 mV) and AA content was lower than the AMPS content, as confirmed from the XRD pattern. Thus, from the above result, the anionic-exchange ability of AMPS was higher than that of AA, which leads to the positive charge density of AA–HT being higher than that of AMPS–HT. Hence, inter- or intramolecular ionic bonding ability of the A-series gels was greater than that of the S-series gels, causing lower water absorbency of the A-series than that of the S-series gels.

From the figures, we also found that the water absorbency, measured by the tea-bag method, is greater than that measured by the suction method. Because the water absorbency is attributed primarily to the water absorbed by the gels and the free water residing between the gel particles, the smaller degree of absorbency by suction is attributed primarily to the scarcity of free water between the gel particles.

### Water absorbency in various saline solutions

The water absorbencies for poly(NaA/AMPS–HT) (S3) and poly(NaA/AA–HT) (A3) copolymeric gels, as a function of different ionic strengths for $NaCl_{(aq)}$, $CaCl_{2(aq)}$, and $FeCl_{3(aq)}$, are shown respectively in Figures 4–6. Figures 4 and 5 show that the water absorbencies, for the copolymeric gels in various salt solutions, decrease with increasing ionic strength of salt solutions. This can be attributed to the cations in the salt solution such as $Na^+$, $Ca^{2+}$, and $Fe^{3+}$. The cation would neutralize the carboxylate group. The difference in ionic osmotic pressure, between the gel and the external solution, reduces with increasing ionic strength of the salt solutions. Thus, the water absorbency decreases when the ionic strength in the external solution increases. Water absorbency curves for monovalent cationic salt solution were flatter than those for divalent and trivalent cationic salt solutions. The water absorbency converged to zero when those gels were immersed in a high ionic strength divalent or trivalent cationic salt solution, but not for monova-

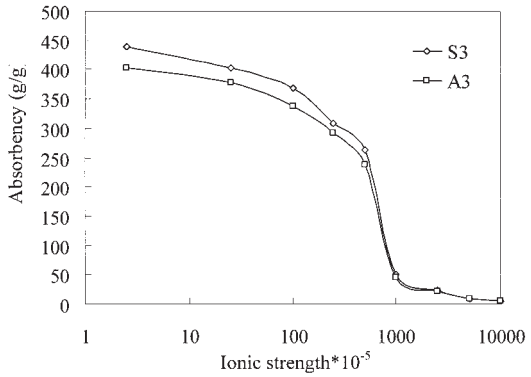


**Figure 6** Water absorbency for 3 wt % sample of the different copolymeric gels in the $CaCl_{2(aq)}$ with various ionic strengths.

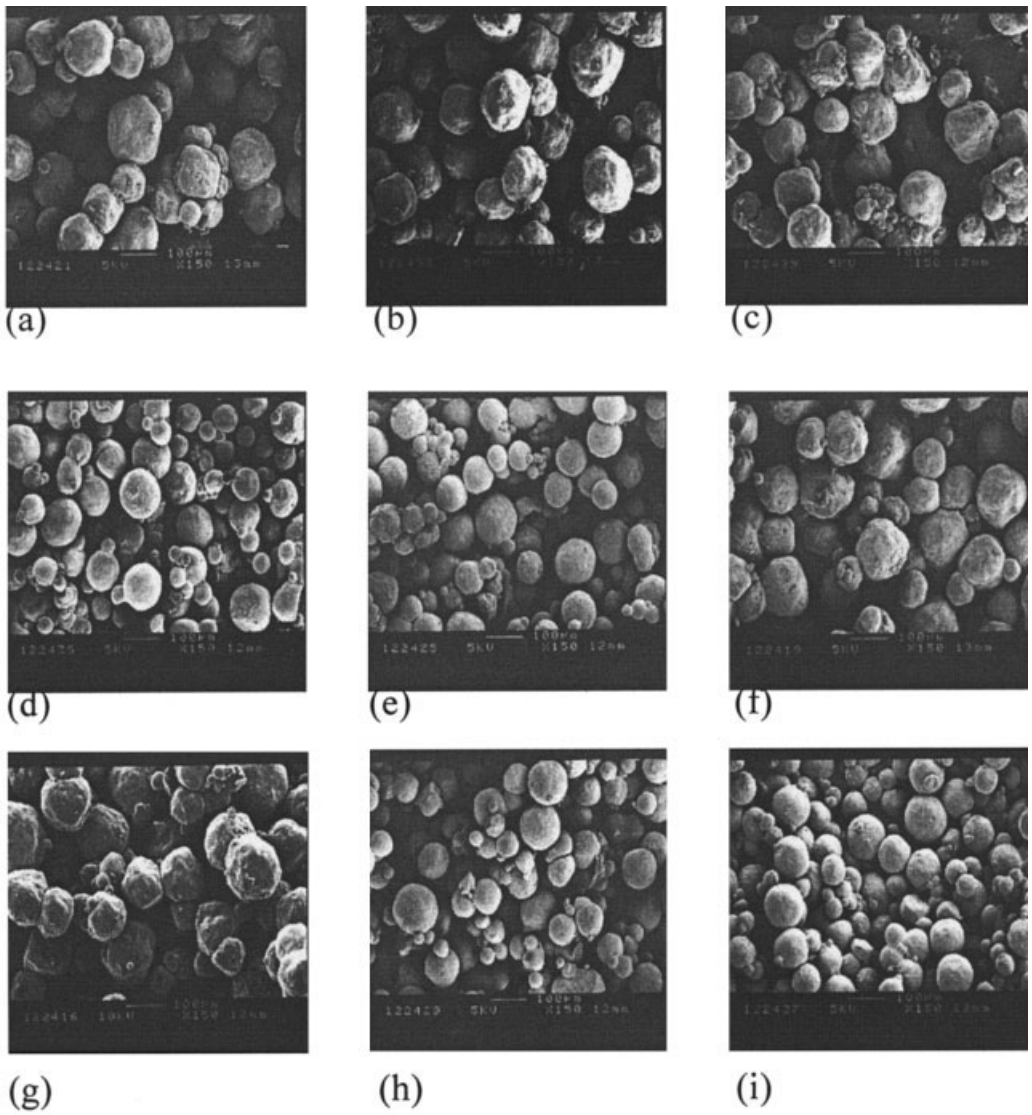


**Figure 7** Scanning electron micrograph for dried IHT series gels (×150): (a) S0, (b) S1, (c) S3, (d) S5, (e)S7, (f) A1, (g) A3, (h) A5, and (i) A7.

lent cationic salt solution. This is because the divalent calcium ion ($Ca^{2+}$) and trivalent ferric ion ($Fe^{3+}$) form complexes with the carboxylate group.[37]

In addition, the result in Figure 6 indicates that the water absorbency curve for poly(NaA/AA–HT) (A3) was flatter than that for poly(NaA/AMPS–HT) (S3) because the positive charge density of AA–HT was higher than that of AMPS–HT: absorption of cations of salt ions onto the surface of AA–HT is thus hindered. Thus, the decreased range of the water absorbency, for the poly(NaA/AMPS–HT), was greater than that for the poly(NaA/AA–HT).

## SEM

Microphotographs of the particles for two series of nanocomposite superabsorbents are shown in Figure

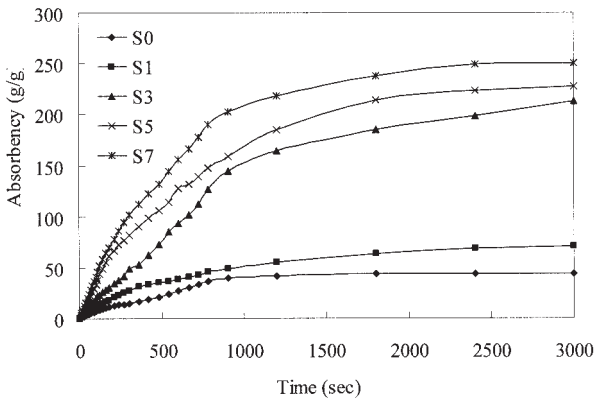


**Figure 8** Absorption rate in deionized water for the AMPS–HT gels by the DW method.

**TABLE II**
**Absorption Characteristics for SA/AMPS–HT and SA/AA–HT Nanocomposite Gels in Deionized Water**

| Condition | S0 | A1 | A3 | A5 | A7 | S1 | S3 | S5 | S7 |
|---|---|---|---|---|---|---|---|---|---|
| Initial absorption rate, $Q$/min | | | | | | | | | |
| 30 s | 5.27 | 6.00 | 9.58 | 15.30 | 22.86 | 6.10 | 13.60 | 19.26 | 24.10 |
| 30 s to 1 min | 4.20 | 4.94 | 6.08 | 12.60 | 13.34 | 5.04 | 11.2 | 13.36 | 32.02 |
| 1–3 min | 3.20 | 3.28 | 8.98 | 10.35 | 22.30 | 5.65 | 9.16 | 22.31 | 23.00 |

7(a)–(i). As shown in the various panels of this figure, the particles obtained from inverse suspension polymerization approach a spherical shape. Results shown in this figure also indicate that the particle sizes for the present gels decrease with increasing content of the IHT in the two series of gels. The different particle sizes will affect their water absorption behavior.

### Effect of IHT content on absorption rate for the copolymeric gels

Buchanan et al.[38] suggested that the swelling kinetics for an absorbent is significantly influenced by swelling capacity, size distribution of powder particles, specific surface area, and apparent density of the polymer.

Figures 8 and 9 show the absorption rate in deionized water for A-series and S-series copolymeric gels. The characteristic absorption data of these two series of gels are shown in Table II. The results, in Table II, indicate that the greater the amount of IHT in gels, the higher the initial absorption rate for poly(NaA/IHT). This is because the hydrated OH group of IHT readily binds water to form a rapid microstream of water, which would enhance the absorption rate for the copolymeric gel. SEM observation showed that the particle size of A-series and S-series gels decreased with increasing content of IHT in gels. For this reason, the initial absorption rate of the two series of gels increased with increasing content of IHT in gels.

From the SEM micrographs, the appearance of A-series gels was similar to that of S-series gels, so the swelling ratio depended on the affinity of the gels for water. Because the water absorbency of A-series gels was lower than that of S-series gels, the initial absorption rate was lower than that for the S-series gels.

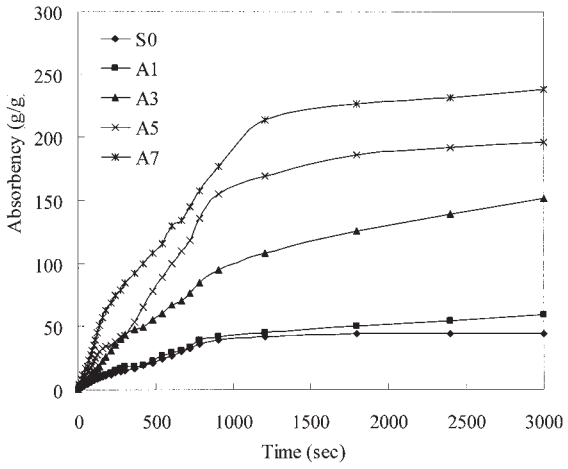


**Figure 9** Absorption rate in deionized water for the AA–HT gels by the DW method.

## CONCLUSION

From the above results, some conclusions can be drawn as follows: the water absorbency of poly(NaA) in deionized water, or in various saline solutions, would be improved by copolymerizing NaA with a small amount of IHT. However, the initial absorption rate was increased, with increasing number of hydrated OH groups of IHT, and increased with a decrease of the particle size. The initial absorption rate of the A-series gels was lower than that of the S-series gels. However, the water absorbency of these gels decreased with increasing ionic strength of external salt solution. The decreased range of the water absorbency, for the poly(NaA/AMPS–HT), was larger than that for the poly(NaA/AA–HT).

The authors gratefully acknowledge financial support of this research provided by Tatung University, Taipei, Taiwan, under Grant B91-1413-01.

## References

1. Sakiyama, T.; Chu, C. H.; Fujii, T.; Yano, T. J Appl Polym Sci 1993, 50, 2021.
2. Yoshida, M.; Asano, M.; Kumakura, M. Eur Polym J 1989, 25, 1197.
3. Shiga, T.; Hirose, Y.; Okada, A.; Kurauchi, T. J Appl Polym Sci 1992, 44, 249.
4. Shiga, T.; Hirose, Y.; Okada, A.; Kurauchi, T. J Appl Polym Sci 1993, 47, 113.
5. U.S. Department of Agriculture. U.S. Pat. 3,981,100 (1961).
6. Taylor, N. W.; Fanta, G. F.; Doane, W. M.; Russell, C. R. J Appl Polym Sci 1978, 22, 1343.
7. Burr, R. C.; Fanta, G. F.; Doane, W. M. J Appl Polym Sci 1979, 27, 2713.
8. Fanta, G. F.; Burr, R. C.; Doane, W. M.; Russell, C. R. J Appl Polym Sci 1979, 24, 1384.
9. Kejun, Y.; Berlian, W. J Appl Polym Sci 1990, 41, 3079.

10. Fanta, G. F.; Burr, R. C.; Doane, W. M. J Appl Polym Sci 1979, 24, 2015.
11. Yoshinobu, M.; Morita, M.; Sakata, I. J Appl Polym Sci 1992, 45, 805.
12. Lokhande, H. T.; Varadarjan, P. V.; Iyer, V. J Appl Polym Sci 1992, 45, 2031.
13. Zoda, I. Funct Mater 1986, 6, 76.
14. Isomi, K. Jpn. Pat. 56,707 (1989).
15. Nagasuna, K.; Suminaga, N.; Kimura, K.; Shimonura, T. Jpn. Pat. 126,234 (1989).
16. Imada, H.; Fujiwaka, M. Jpn. Pat. 141,938 (1989).
17. Fujio, A.; Komae, T.; Yutaka, Y. Jpn. Pat. 210,463 (1989).
18. Yada, S.; Shibano, T.; Ito, K. Jpn. Pat. 215,801 (1990).
19. Sano, M.; Mikamo, H.; Suehiro, T.; Wakabayashi, N. Jpn. Pat. 258,839 (1991).
20. Sakiyama, T.; Chu, C. H.; Fujii, T.; Yano, T. J Appl Polym Sci 1993, 50, 2021.
21. Miyata, S. Clays Clay Miner 1975, 23, 369.
22. Ulibarri, M. A.; Pavlovic, I.; Barriga, C.; Hermosin, M. C.; Cornejo, J. Appl Clay Sci 2001, 18, 17.
23. Sels, B.; Vos, D. D.; Buntinx, M.; Pierard, F.; Mesmaeker, A. K.; Jacobs, P. Nature 1999, 400, 855.
24. Vaccari, A. Catal Today 1998, 41, 53.
25. Yun, S. K.; Pinnavaia, T. J. Chem Mater 1995, 7, 348.
26. Moreyon, J. E.; De, R. A.; Forano, C.; Besse, J. P. Appl Clay Sci 1995, 10, 163.
27. Pavan, P. C.; Gomes, G.; Valim, J. B. Microporous Mesoporous Mater 1998, 21, 659.
28. Hibino, T.; Tsunashima, A. Chem Mater 1998, 10, 4055.
29. Oriakhi, C. O.; Farr, I. V.; Lerner, M. M. J Mater Chem 1996, 6, 10.
30. Liang, L.; Liu, J.; Gong, X. Langmuir 2000, 16, 9895.
31. Lee, W. F.; Fu, Y. T. J Appl Polym Sci 2003, 89, 3652.
32. Carlino, S.; Solid State Ionics 1997, 98, 73.
33. Lee, W. F.; Chen, Y. C. J Appl Polym Sci, to appear.
34. Lee, W. F.; Wu, R. J. J Appl Polym Sci 1996, 62, 1099.
35. Flory, P. J. Principles of Polymer Chemistry; Cornell University Press: Ithaca, NY, 1953.
36. Wu, J. H.; Lin, J. M.; Yang, Z. F.; Pu, M. I. Macromol Rapid Commun 2001, 22, 422.
37. Lee, W. F.; Yang, L. G. J Appl Polym Sci 2004, 92, 3422.
38. Buchanan, K. J.; Hird, B.; Letcher, T. M. Polym Bull 1986, 15, 325.